

GAS AND PLASMA-BEAM DISCHARGES AND THEIR APPLICATIONS

THE ATOMIC-MOLECULAR PROCESSES IN A HYDROGEN PLASMA AT INITIAL STAGE OF A DISCHARGE

V.B. Yuferov, E.I. Skibenko, V.I. Tkachov, V.V. Katrechko, A.S. Svichkar
National Science Center “Kharkov Institute of Physics and Technology”, Kharkiv, Ukraine
E-mail: v.yuferov@kipt.kharkov.ua

For 0-dimensional the task of a hydrogen plasma formation at initial stage of a charge is considered. For these conditions the dynamics of atomic and molecular ions density and energy balance in a hydrogen plasma are considered.

PACS: 52.50.Qt, 52.55.Hc

INTRODUCTION

In recent times, significant progress has been made in obtaining pure plasma in thermonuclear installations, and if a few years ago the concentration of impurities in the plasma reached 5...10% and effective plasma charge Z_{eff} was at the level 3...8, now the concentration of impurities is reduced to ~ 0.1...1% and Z_{eff} to 1...1.5; at the same the plasma temperature also increased [1, 2]. This progress is associated with identifying the main sources of pollution, and the use of measures to reduce the flow of impurities. It has been shown in experiments that even in a well-cleaned system, impurities enter the plasma already at the first stage of the discharge, when breakdown occurs and the plasma touches the walls. In this case, impurities enter the plasma due to several mechanisms, the main ones are unipolar arcs and ion-stimulated desorption. The specific impurity yield in both processes is very high and these mechanisms can create a significant initial impurity concentration. For example, according to [3] Z_{eff} is 3 and 7, respectively in modes with and without divertor, through 0.1...0.15 s after the start of the discharge, there are both light and heavy impurities. The further course of the impurity concentration determines by the processes of their transport in the plasma and the boundary. At the time of ~0.5 s after the start of the discharge, the plasma is purified from impurities up to $Z_{eff} \sim 1$ when the divertor is working, and ~1.3...1.5 in the divertorless case. A similar course was observed in other installations, with sources of impurities in the stationary phase being desorption (light impurities) and spraying or self-spraying (heavy) stimulated by fast ions and neutrals. In the theoretical consideration of the impurities entering the plasma, usually, the stimulated desorption and spraying are taken into account [4, 5].

It should be noted two areas of work. The first is to determine the flow of impurities to the plasma boundary with its subsequent averaging over the entire volume, which gives an average concentration of impurities in the plasma. Such calculations are carried out in a 0-dimensional approximation in order to study and compare the characteristics of various wall materials and the specific contribution of various erosion mechanisms. Secondly, for a given impurity flux onto the plasma boundary, the concentration distribution or charge composition of the impurity in a plasma of a given density and temperature is determined (one or two-dimensional

approximation is used to study plasma confinement and energy balance). Both approaches have a fairly good quantitative agreement with the experiment in the stationary phase of the discharge, but do not explain the burst of light impurities at the initial stage of the discharge. The exclusion of the initial stage of discharge from consideration does not allow a complete analysis, although at this time there are no flows of highly energetic charge-exchange atoms that have a high erosion coefficient K_i in both light and heavy impurities. At the same time, at the initial stage, there are large flows of atomic hydrogen F_h and ultraviolet radiation with significant erosion ability with respect to light impurities, which is especially important for systems with insufficiently good cleaning of surfaces and for attached volumes, from which contamination of the initially cleaned surface through the gas phase can occur. Light impurities that fall into the discharge at the initial stage are almost completely captured by the plasma and heated together with the main component. However, they can become the main cause of the appearance of heavy impurities. This situation may be relevant for stellarator – type systems in which magnetic diaphragm isolates the place of formation of the plasma filament away from the walls, and in the presence of the divertor [6, 7], when the angles separatrix not rely on the material wall and formation unipolar arcs at these locations is difficult or impossible.

The above is confirmed by many experiments. But we are interested in the situation that was not practically provided by the latter due to the lack of data on complex polyatomic molecules present in spent nuclear fuel – SNF and, accordingly, a multicomponent oxide plasma in which chemical reactions can take place. That is, hydrogen plasma with impurities is a kind of simulation environment, allowing you to look at the spent nuclear fuel plasma from the view of atomic-molecular processes in SNF plasma formed mainly from actinide oxides supplemented with a mixture of oxides of lanthanides, zirconium, molybdenum, etc. [8].

INITIAL STAGE OF DISCHARGE

The initial stage of plasma formation in the closed magnetic traps viewed in several studies [9 - 11], for simplicity only hydrogen atoms. In [9], a one-dimensional model of gas breakdown in a tokamak was considered, leading to reasonable estimates of the ioni-

zation time and its dependence on the basic parameters of the plasma. The existence of a critical electric field has been established, above which there is observed a skinning of the discharge current, below it is a quasi-uniform current distribution. The dependences of the electron temperature T_e on the gas ionization time are given, from which it follows that in a certain region of the discharge time from $5 \cdot 10^{-5}$ s to $0.5 \cdot 10^{-3}$ s (plasma density from $10^2 n_e$ to $0.8 n_e$) the temperature can remain constant, for example, about 5 eV. In [10, 11], in the 0-dimensional approximation (homogeneous distribution of current and plasma density), a scenario of operation of tokamak-type facilities was considered. It is shown that under different scenarios – both during current breakdown (ohmic heating) and at RF or microwave initial discharges – the electron temperature can remain for a long time 10...50 ms as the plasma density increases to $5 \cdot 10^{13}$ cm $^{-3}$ at the level of 2...15 eV. However, the simplification in these calculations, associated with a hypothetical situation, when ionizing atomic hydrogen filling the discharge chamber without interacting with the walls occurs, does not allow us to consider the problem associated with the appearance of light impurities at the initial stage of discharge, and correctly estimate the power losses that are needed to create a plasma. In contrast to our predecessors, we were interested in the amount of light impurity streams associated with the flows of photons and hydrogen atoms F_{ph} and F_h and entering the plasma boundary, the average density of impurities that could be reached by the time of the heating stage, as well as the role of vacuum conditions. In contrast to our predecessors, we were interested in the magnitudes of streams of light impurities associated with the flows of photons and hydrogen atoms and entering the plasma boundary, the average density of impurities that could be reached by the time of the heating stage, and the role of vacuum conditions. The main conditions for solving the problem were:

- multicomponent composition – protons, molecules, molecular ions;
- at the initial stage there is no ion heating, $T_i \ll T_e < 10 \dots 15$ eV;
- the constancy of the electron temperature at the ionization stage.

This simplified the task, although a programmed case is possible with the dependence of temperature on time correlated with the input of power into the discharge, the maximum plasma density $n_e = 2 \cdot 10^{13}$ cm $^{-3}$ according to [12]. When the condition of constant number of particles in the system initial density of molecular hydrogen $n_2 = 1 \cdot 10^{13}$ cm $^{-3}$. In experimental systems it is achieved after a large number of pulses, when the hydrogen recycling rate at the wall is close to 1, or by introducing an additional gas flow which compensates losses in the walls.

To determine the role of chemical and photodesorption in the process of impurities in the plasma boundary is sufficient 0-dimensional approximation. This is explained by the fact that the flow of impurities from the wall, determined by the fluxes of photons and hydrogen atoms, practically does not depend on the place of their appearance, since the photons are not absorbed by the plasma, and the path length of the hydrogen atom before

ionization, even at maximum density, is much larger than the system dimensions. In addition, the characteristic times for the growth of the plasma density, or growth times for the average density of impurities more than an order of the value greater than time of hydrogen atoms flow in the system.

	Processes	Sections
$H_2^0 + e$	$H_2^+ + 2e$	σ_1
	$H_1^+ + H_1^0 + 2e$	σ_2
	$2H_1^0 + e$	σ_3
$H_2^+ + e$	$H_1^+ + H_1^0 + e$	σ_4
	$2H_1^+ + 2e$	σ_5
	$2H_1^0$	σ_6
$H_1^0 + e$	$H_1^+ + 2e$	σ_7
$H_2^+ + H_2^0$	$H_3^+ + H_1^0$	σ_8
$H_3^+ + e$	$2H_1^0 + H_1^+ + e$	σ_9
	$3H_1^0$	σ_{10}
$H_1^0 + e$	$H_1^+ + e$	σ_{11}
$H_2^0 + e$	$H_2^+ + e$	σ_{12}
	$H_1^+ + H_1^0 + 2e$	σ_{13}

* Excited atoms and hydrogen molecules

It should be immediately noted that in order to determine the radial distribution of the density of impurities, at least a one-dimensional approximation is necessary. Moreover, it can be applied only to one equation that relates the concentration of impurities with their flow. This is beyond the scope of our tasks. However, it is clear from simple considerations that, due to the low speeds of the passage of impurity molecules coming from the walls at thermal velocity and significant ionization cross sections of the mean free path of impurity molecules before ionization at plasma densities above 10^{12} cm $^{-3}$ become smaller than the system size, i.e. during the plasma density increase, impurities begin to be trapped in an increasingly thin surface layer, reaching about 1 cm at the end of the ionization stage. And for the characteristic time t_n – growth of plasma density, they do not have time to diffuse into the plasma at a considerable distance. Even with $D_z = 4 \cdot 10^3$ cm 2 /s taken in [11] for hot plasma $\Delta r = \sqrt{D t_n} = 2$ cm. However, in the process of heating, as is well known, impurities are fairly quickly transported deep into the plasma, so the operation of averaging impurities over the entire volume, used in the 0-dimensional approximation, gives essentially the initial (not zero) impurity concentration at the beginning of the stationary phase. As mentioned earlier in [1 - 4], it is from the moment of the end of heating that the process of accumulation of impurities in the plasma begins, as a result of other erosion processes.

The main processes occurring in a hydrogen plasma and determining its charge and component composition are presented in Table. The initial stage of the dis-

charge, as well as the subsequent stationary phase, can be described by the following system of differential equations (1) - (11), which allows determining the time variation in the discharge chamber of the electron density n_e , atomic hydrogen n_i , hydrogen molecules n_2 , ions H_1^+ , H_2^+ , H_3^+ respectively n_1^+ , n_2^+ , n_3^+ , plasma production powers W_p ionization of gas P_{ion} , atomic hydrogen and photon fluxes to the wall F_h and F_{ph}^j , where j - is

$$\frac{dn_1}{d\tau} = n_e \left[n_2 (\sigma_2 + 2\sigma_3) + n_2^+ (\sigma_4 + 2\sigma_6) + n_3^+ (2\sigma_9 + 3\sigma_{10}) - n_1\sigma_7 \right] + n_2 n_2^+ \sigma_8 - \frac{n_1}{\tau_1} - \sum_{m=1}^{\infty} \alpha_m \beta_m \frac{n_1}{\tau_1}, \quad (2)$$

where m - is the number of collisions of a hydrogen atom with a wall before recombination.

$$\frac{dn_2}{d\tau} = -\frac{d}{d\tau} \left(\frac{1}{2} n_1 + \frac{1}{2} n_1^+ + n_2^+ + \frac{3}{2} n_3^+ \right), \quad (3)$$

$$\frac{dn_1^+}{d\tau} = n_e (n_2 \sigma_2 + n_2^+ (\sigma_4 + 2\sigma_5) + n_1 \sigma_7 + n_3^+ \sigma_9) - \frac{n_1^+}{\tau_p}, \quad (4)$$

$$\frac{dn_2^+}{d\tau} = n_e (n_2 \sigma_1 - n_2^+ (\sigma_4 + \sigma_5 + \sigma_6)) - n_2 n_2^+ \sigma_8 - \frac{n_2^+}{\tau_p}, \quad (5)$$

$$\frac{dn_3^+}{d\tau} = n_2 n_2^+ \sigma_8 - n_3^+ n_e (\sigma_9 + \sigma_{10}) - \frac{n_3^+}{\tau_p}, \quad (6)$$

$$\frac{dW_p}{d\tau} = P_h - P_{ion} - P_r - P_{rad} - \frac{W_p}{\tau_E}, \quad (7)$$

$$W_p = \frac{3}{2} k n_e [T_e + T_i] V_p, \quad (8)$$

where P_h , P_{ion} , P_r , P_{rad} going to plasma heating, ionization, recharging, emission of impurities; V_p - plasma volume; k - is the Boltzmann constant.

$$n_1^+ + n_2^+ + n_3^+ - n_e = 0, \quad (9)$$

$$P_{ion} = n_e \left[\begin{aligned} & n_2 (\sigma_1 E_1 + \sigma_2 E_2 + \sigma_3 E_3) + n_2^+ (\sigma_4 E_4 + \sigma_5 E_5 + \sigma_6 E_6) + \\ & + n_1 \sigma_7 E_7 + n_3^+ (\sigma_9 E_9 + \sigma_{10} E_{10}) + n_1 \sigma_{12} E_{12} + n_2 \sigma_{13} E_{13} \end{aligned} \right], \quad (10)$$

$$P_{rad} = \sum n_z \langle \sigma v \rangle_z E_z, \quad (11)$$

E_i - the amount of energy loss in this process.

The values of the plasma particle lifetime $\tau_p=10...20$ ms, determined through the energy plasma lifetime τ_E ($\tau_p \approx 3\tau_E$), taken neoclassical [13] with a magnetic field $B = 2$ T, $a = 13.5$ cm, $R=100$ cm; $t = 0.6$ s [12]. For the real system, we are interested in the time of the creation of the plasma is not more than 1 ms, so the members of the energy loss and the plasma particles during this time is negligible.

The lifetime of hydrogen atoms before going on the wall $\tau_1 = a/\mathcal{G}_1$, where \mathcal{G}_1 - is the average velocity of hydrogen atoms with allowance for multiple collisions with the wall before recombination or ionization. The energy of the hydrogen atoms produced during the dissociation of hydrogen molecules and molecular ions is in the range of an electron volt to 12 eV with maxima in the region of 4...6 eV [14 - 16]. There are no exact data on the values of the reflection coefficients of particles α and the energy β of the energy range below 10 eV. In [17, 18], the reflection coefficients were calculated for an energy $E > 10$ eV, and experimental data are available only for $E > 100$ eV. Extrapolation of the values of α and β in the energy range of less than 10 eV gives values of 0.7...0.9. In this case, the average energy of hydrogen

the photon energy; the time variation of the concentration of light impurities averaged over the entire volume of n^c , n^o - carbon and oxygen.

$$\frac{dn_e}{d\tau} = n_e \left[n_2 (\sigma_1 + \sigma_2) + n_2^+ (\sigma_5 + \sigma_6) + n_1 \sigma_7 - \frac{1}{\tau_p} \right], \quad (1)$$

atoms is ≈ 2 eV. I.e. the correction factor before the value of the flow of atomic hydrogen onto the wall as a result of multiple collisions turns out to be 3...3.3. It should be noted that in all equations, for simplicity, the quantity $\langle \sigma v \rangle_i$ replaced by σ_i .

As initial conditions are taken: $n_2=1 \cdot 10^{13}$ cm⁻³, $n_e=1 \cdot 10^{11}$ cm⁻³, $n_1^+=5 \cdot 10^{10}$ cm⁻³, $n_2^+=4 \cdot 10^{10}$ cm⁻³, $n_3^+=1 \cdot 10^{10}$ cm⁻³, which in real devices are easily achieved with the help of low-power pre-plasma systems.

Due to the relatively low coefficient of impurity reuptake by surfaces lying at the level of 0.05...0.3 [19], low gas-kinetic velocities at the level of $5 \cdot 10^4$ cm/s and high ionization cross sections, impurities desorbed from the walls are ionize, dissociate and, thus, are captured by the plasma with density $n_e > 1 \cdot 10^{12}$ cm⁻³. For the case of [12], the mean time of passage of impurities from the wall to the wall is $\tau = a/\mathcal{G}_{np} \approx 270$ ms and the mean free path of the impurity before ionization at $n_e = 1 \cdot 10^{12}$ cm⁻³ and $T_e = 6$ eV, $\lambda = 10$ cm.

Analysis of equations (1) - (6) shows that the plasma electron density increases exponentially with time $n_e(t) = n_e(0)e^{at}$. The exponent $a = n_2 \sigma_1 + n_2^+ (\sigma_5 + \sigma_6) + n_1 \sigma_7 - 1/\tau_p$ depends on time, decreasing as n_2 burns out, n_2^+ grows. However, for a long time, n_2 changes little and the density increases by a factor of e over time $t = 1/(n_2 \sigma_1)$, since n_2^+ and n_1 are small, i.e. at a given density n_2 the plasma density growth rate n_e is determined by the value σ_1 , the value of which, for example, for T_e , values equal to 3, 4, 6, and 12 eV, is respectively $1 \cdot 10^{-10}$; $3.8 \cdot 10^{-10}$; $1.5 \cdot 10^{-9}$, and $9 \cdot 10^{-9}$ cm⁻³·s⁻¹. Since the ionization rates for the σ_1 and σ_7 processes are close in a wide temperature range T_e , the initial speed of creating the plasma using atomic and molecular components at the same concentrations n_1 and n_2 are equal, and that allowed the authors of [9 - 11] to obtain reasonable ionization times.

However, to achieve the same final plasma density, the concentration must be twice as high as n_2 , which in the latter case reduces the plasma formation rate by half. The plasma formation rate will be reduced due to the second term, since $\sigma_6 \gg \sigma_5$, and the concentration of growth n_1 (third member) at $\sigma_1 = \sigma_7$ compensates for this decrease. In Fig. 1 shows the dependences $n_e = f(t)$ or four temperatures: 3, 4, 6, and 12 eV. As can be seen from equations (1) - (6), the density increase n_2^+ and n_3^+ is limited long before reaching the maximum density n_e , where

$$n_2^+ (\text{max}) = \frac{n_e n_2 \sigma_1}{n_e (\sigma_4 + \sigma_5 + \sigma_6) + n_2 \sigma_8}, \quad (12)$$

$$n_3^+ (\text{max}) = \frac{n_2 n_2^+ \sigma_8}{n_e (\sigma_9 + \sigma_{10})}. \quad (13)$$

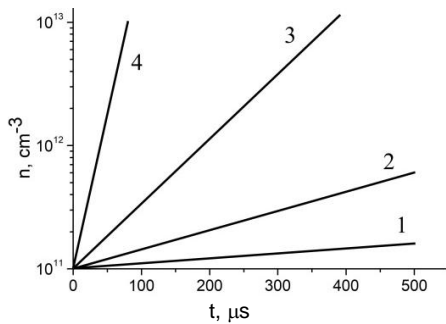


Fig. 1. The dependence of plasma density on time for different values of electron temperature: 1 – $T_e=3$; 2 – $T_e=4$; 3 – $T_e=6$; 4 – $T_e=12$ eV

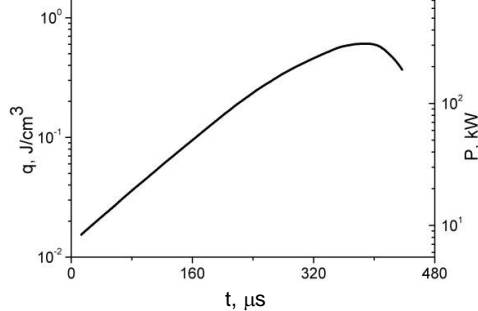


Fig. 2. The time distribution of the specific energy consumption for ionization and excitation. (To the right, the ordinate shows the total energy consumption for a system similar to [12])

Note that presented in Fig. 2 the energy consumption for electronic excitation and ionization is less than real, in which oscillatory processes should be taken into account, especially strong at temperatures less than 4 eV, and which can be a significant value at $T_e > 4$ eV.

Due to the presence of two terms in the denominator with n_e and n_2 the maximum for n_2^+ is quite wide. The value of W_p – energy consumption for the creation of a plasma grows exponentially, like n_e . At the same time P_r and W_p/τ_E are small, and P_{rad} increases from 0 for $n^c=0$ to $0.08P_{ion}$ at $n^o+n^c=0.02n_e$ (see Fig. 2).

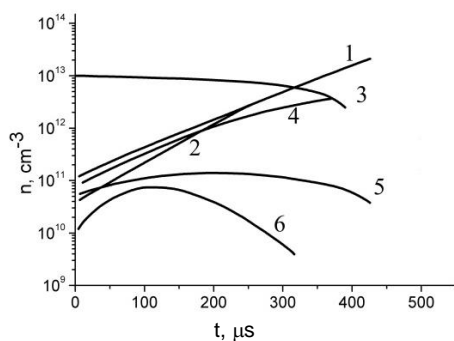


Fig. 3. The time distribution of the electron density of plasma (1), protons (2) of hydrogen molecules (3), hydrogen atoms (4) of molecular ions H_2^+ (5) and H_3^+ (6) for an electron temperature of 6 eV

With an exponential growth of W_p value T_e can remain constant, grow or fall, but at $T_e < 10$ eV, as can be seen from σ_1 , a change in T_e by 1...2 eV sharply increases ionization losses, therefore in real systems $T_e = \text{const}$ is often observed. In general, as mentioned above, the course of $W_p(T_e)$ is determined by the necessary discharge scenario, as well as by the possibilities of the energy input (Fig. 3).

CONCLUSIONS

As can be seen, the growth rate of plasma density is mainly determined by the value of ionization cross section. The increase in energy consumption is determined by ionization losses, since the selected electron temperatures provide low energy costs for vibrational levels. At the time of 200...400 μs , the “burnout” of H_2^+ and H_3^+ ions begins, respectively.

For a number of molecules of non-electronegative gases at the electron temperature $T_e=1...3$ eV the main fraction of the discharge energy input focuses specifically on the excitation of the vibrational degrees of freedom of the ground electronic states.

REFERENCES

1. A Gibson. Impurity behaviour in real simulated tokamak plasmas // *J. Nucl. Mat.* 1978, v. 76, p. 92-102.
2. G.M. Cracken et al. Time resolved metal impurity concentrations in the DITE tokamak using RBS analysis // *J. Nucl. Mat.* 1978, v. 76, p. 431-436.
3. M. Keilhacker et al. Impurity control experiments in the ASDEX divertor tokamak. Report on 8 Intern // *Conf. on Plasma Physics and Control. Nuclear Fusion Research.* 1980, Brussels, Belgium.
4. D. Duchs, G. Haas, D. Pfirsch, H. Vernicel. On the impurity problem in quasi-steady STABE toroidal plasma experiments and fusion reactors // *Conf. on Surface Effects in Controlled Thermonuclear Fusion Devices and Reactors.* 1974, Argonne, Nat. Lab. Argonne, USA.
5. S.J. Fielding, A.D. Sanderson. The calculation of recycling and impurity evolution in tokamak // *J. Nucl. Mat.* 1980, v. 93/94, p. 441.
6. G.G. Lesnyakov, Yu.V. Kholod, V.B. Yuferov. Work features and gas efficiency of the torsatron divertor system "Uragan-3" // *Problems of Atomic Science and Technology. Series "General and Nuclear Physics"*. 1981, v. 1, p. 102.
7. V.S. Voitsenya, E.D. Volkov, Yu.A. Gribanov, et al. On the interaction of plasma with the surface in magnetic traps of the stellarator type // *Problems of Atomic Science and Technology. Series "Thermonuclear Fusion"*. 1980, v. 2(6), p. 21-28.
8. V.B. Yuferov, S.V. Shariy, T.I. Tkachova, V.V. Katrechko, A.S. Svichkar, V.O. Ilichova, M.O. Shvets, E.V. Mufel. Calculations of Ion Trajectories at Magnetoplasma Separation and Experiments with Polyatomic Gases // *Acta Polytechnica.* 2017, № 57(1), p. 71-77, doi: 10.14311/AP.2017.57.0071.
9. V.A. Abramov, V.V. Vikhreev, O.P. Pogutse. The initial stage of development of the discharge in tokamak // *Plasma Physics.* 1977, iss. 3, v. 3, p. 512.
10. Yu.K. Kyznethov, S.A. Lebedev, O.S. Pavlichenco. *Initial stage of discharge in a tokamak with a poloidal divertor:* Preprint KIPT 79-31. Kharhov: KIPT AS USSR, 1979, p. 18.
11. *IHTOR: Zero phase report of the Intern. Tokamak Reactor Workshop.* 1980, Vienna, 5-16 Feb., 10-19 December 1979. International Atomic Energy Agency, Vienna.

12. E.D. Volkov, A.V. Georgievskij, A.G. Dikij, et al. *Basic physical installation tasks "Uragan-3"*: Preprint KIPT 81-45. Kharhov: KIPT AS USSR, 1981, 28 p.
13. A.A. Galeev, P.Z. Sagdeev. *Neoclassical diffusion theory*. M.: "Questions of plasma theory. Atomizdat", 1973, v. 7, p. 210-271.
14. M. Misakian, J. Zorn. Dissociative excitation of molecular hydrogen by electron impact // *Phys. Rev.* 1972, v. 6A, № 6, p. 446.
15. B.L. Carnahan, E.S. Zipf. Dissociative excitation of H₂, HD and D₂ by electron impact // *Phys. Rev.* 1977, v. 16A, № 3, p. 991.
16. G.N. Polyakova, A.I. Ranyuk, V.F. Erko. Distributions of the kinetic energies of excited atoms arising during dissociation // *JETP*. 1977, iss. 73, v. 6(12), p. 2131.
17. W. Eckstein, H. Verbeck. Reflection of H, D and He from C, Ti, Ni, Mo, W, Au // *J. Nucl. Mat.* 1978, v. 76/77, p. 365-369.
18. O.S. Oen, M.T. Robinson. Computer simulation of the reflection of hydrogen and the sputtering of hydrogen from metal hydrides // *J. Nucl. Mat.* 1976, v. 63, p. 210; *J. Nucl. Mat.* 1978, v. 76/77, p. 370-377.
19. G.M. Cracken, P.E. Stott. *Plasma-surface interactions in tokamaks*. Abingdon: Preprint CLM, Culham Laboratory, Oxfordshire, 1979, p. 573.
20. Yu.S. Kulyk, V.E. Moiseenko, T. Wauters, A.I. Lysoivan. A numerical model of radio-frequency wall conditioning for steady-state stellarators // *Problems of Atomic Science and Technology. Series "Plasma Physics"*. 2016, № 6, p. 56-59.
21. Yu.S. Kulyk, V.E. Moiseenko, T. Wauters, A.I. Lysoivan. Radio frequency wall conditioning for steady-state stellarators // *Problems of Atomic Science and Technology. Series "Plasma Physics"*. 2018, № 6, p. 46-49.

Article received 25.06.2019

АТОМАРНО-МОЛЕКУЛЯРНЫЕ ПРОЦЕССЫ В ВОДОРОДНОЙ ПЛАЗМЕ НА НАЧАЛЬНОЙ СТАДИИ РАЗРЯДА

В.Б. Юферов, Е.И. Скибенко, В.И. Ткачев, В.В. Катречко, А.С. Свичкар

В 0-м мерном приближении рассмотрена задача создания водородной плазмы на начальной стадии разряда. Для этих условий рассматриваются динамика плотности атомарных и молекулярных ионов водорода и энергетика процесса.

АТОМАРНО-МОЛЕКУЛЯРНІ ПРОЦЕСИ У ВОДНЕВІЙ ПЛАЗМІ НА ПОЧАТКОВІЙ СТАДІЇ РОЗРЯДУ

В.Б. Юферов, Є.І. Скібенко, В.І. Ткачов, В.В. Катречко, О.С. Свічкач

У 0-вимірному наближенні розглянуто задачу створення водневої плазми на початковій стадії розряду. Для цих умов розглянуто динаміку щільності атомарних і молекулярних іонів водню та енергетику процесу.